Fluorescence XAFS Analysis of Some Industrial Materials

BL16B2 and BL16XU, named “SUNBEAM”, are contract beamlines constructed by an Industrial Consortium of 13 companies in cooperation with JASRI in 1999 [1]. We, representing seven interested companies [2] in the consortium, have frequently made the opportunity to measure various industrial materials in cooperation by offering our skills to each other.

During the first semester of 2001, we performed a fluorescence XAFS analysis of certain industrial materials, such as semiconductor devices, catalysts, fluorescent substances, and fuel cells using a Lytle detector [3] at **BL16B2**. Here, we report the results of the analysis of SiGe thin films for a narrow band gap semiconductor device, Lanthanum Manganese oxides for a solid oxide fuel cell.

SiGe film, which is a narrow band gap thin film semiconductor material, is being researched for use in high electron mobility semiconductor materials and infrared sensors. This material can be amorphous, microcrystalline or a mixture of these states, according to fabrication conditions. We attempted local structure analyses by XAFS, because the electronic and optical properties of SiGe films are significantly affected by their structural conditions. An amorphous Ge (a-Ge) film and three microcrystalline SiGe (μc-SiGe) films, which have different Si/Ge compositions, were examined. The Ge concentration was determined by X-ray photoelectron spectroscopy (XPS). Each film (about 0.5 μm in thickness) was fabricated on a glass substrate.

Figure 1 shows a schematic drawing of a microcrystalline material that consists of an amorphous region and microcrystalline regions. The μc-SiGe films which we measured have similar structures to those in Fig. 1, and the grain size was within the range of 10 to 20 nm.

The XAFS measurements were performed using a Lytle detector, since the counting rate of solid state detectors (SSD) is insufficient for these samples. A Ga filter was set in front of the ionization chamber of the Lytle detector to reduce the scattering X-rays. Kr was used as an ionization gas.

Figure 2 shows the Fourier transforms (RDF) of the EXAFS spectra for each sample. The difference between the distance to the first neighbor atom of crystalline Si and that of crystalline Ge is 0.1 Å, and those of SiGe are thought to be within this range.

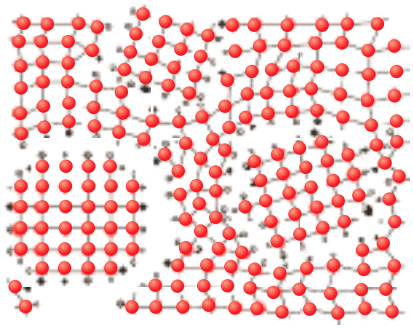

Fig. 1. Schematic drawing of microcrystalline material (provided by National Institute of Advanced Industrial Science and Technology).

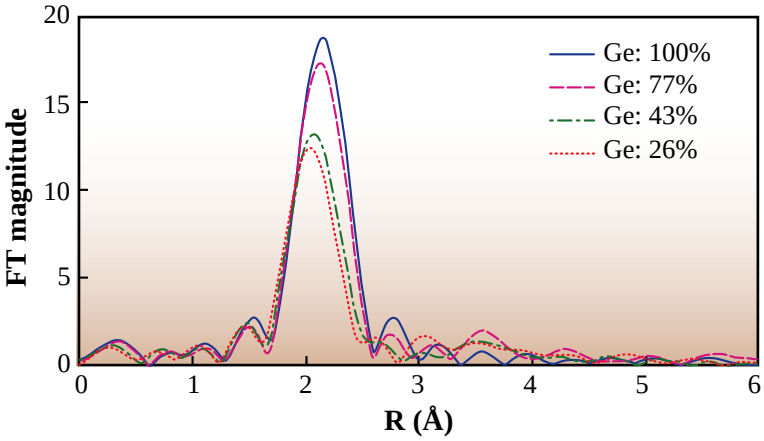

Fig. 2. Fourier transforms of k^3-weighted Ge K-edge EXAFS spectra of SiGe films.

The figure reveals that the distance is longer as the Ge concentration increases within less than 0.1 Å. This method provides excellent radial resolution for these kinds of thin film materials.

In Fig. 3, the distance values to the first neighbor atom derived from a curve-fitting analysis of XAFS spectra were plotted against Ge concentration. The distance values derived from powder X-ray diffraction (XRD) data for crystalline Si and Ge were also plotted. There is a tendency for the distance derived from XAFS to be longer than the average distance between crystalline Si and Ge.

XAFS observes both microcrystalline and amorphous regions, and the distance values by XAFS reveal the average values of both regions. Generally, the bond length of amorphous material is longer than that of crystalline material. Therefore, our XAFS results suggest that the SiGe materials contain both amorphous regions and crystalline regions. On the other hand, crystallographic analyses observe only crystalline regions. We believe a combination of Lytle detector based XAFS and crystallographic analyses can determine the structure of microcrystalline thin film materials.

The perovskite-manganites are technologically important materials as electro-catalysts and electrode materials for high temperature fuel cell applications. Their electronic, catalytic and magnetic

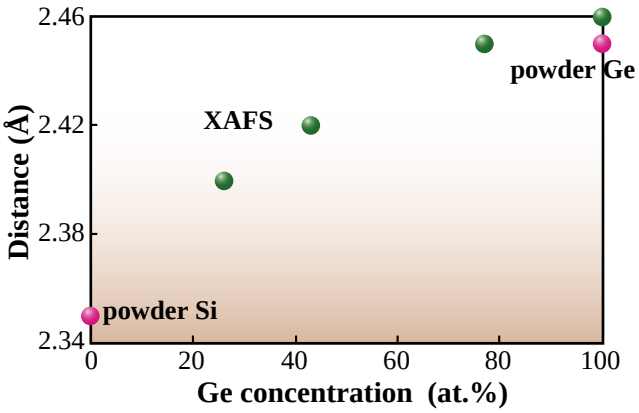

Fig. 3. Distance to the nearest atom taken by XAFS and powder diffraction.

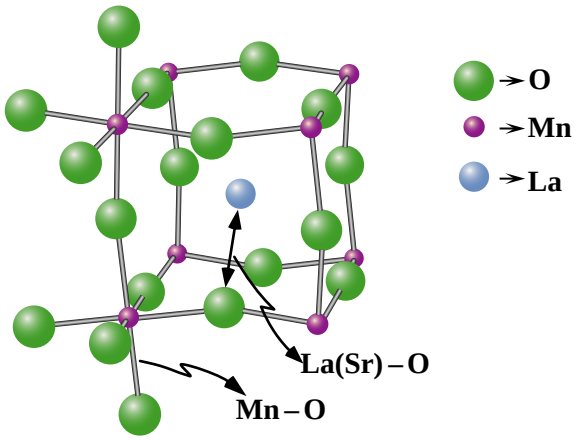

Fig. 4. Schematic drawing of crystal structure of perovskite-type Lanthanum Manganese oxide.

properties are of intrinsic interest, since the crystal and electron structure are changed by the constituted elements. The Lanthanum Manganese oxide, $LaMnO_3$, is semiconductor and has orthorhombic lattice (Pbnm), whereas Sr-doped solid-solutions $La_{1-x}Sr_xMnO_3$ have rhombohedral lattice (R-3c) and their electrical properties around room temperature varies from semiconducting to metallic behavior in the composition range between x = 0.3 and 0.4. A schematic drawing of $LaMnO_3$ is shown in Fig. 4. Recently, we characterized the temperature dependence of the electrical properties of $La_{1-x}Sr_xMnO_3$ and their crystal structure by X-ray Rietveld analysis. However, the role of Sr in La-site, which occupies the crystallographically equivalent site, is not yet clear. In this study, XAFS spectra near the Mn, Sr and La-*K* edge of the $LaMnO_3$ and $La_{1-x}Sr_xMnO_3$ solid-solutions were measured by the fluorescent X-ray method using a Lytle-detector.

The $LaMnO_3$ and $(La_{1-x}Sr_x)MnO_3$ ($0.1 \leq x \leq 0.4$) solid solutions respectively have an orthorhombic $GaFeO_3$-type (Pnma) and a rhombohedral $LaAlO_3$-type (R-3c) structure. Although a slight change of threshold energy in the Mn-*K* edge was observed, the obvious difference was not seen to the XANES spectrum of La(*K*), Sr (*K*) and Mn(*K*)-edge in these

solid solutions. Figure 5 shows the Fourier transforms (RDF) of $La_{0.7}Sr_{0.3}MnO_3$ compound at Mn-*K* edge. The RDF derived from the fluorescent X-ray method agrees with that of the transmitted X-ray method.

Figure 6 shows the composition dependence of La-O, Sr-O and Mn-O distances obtained by XAFS analysis, together with La(Sr)-O and Mn-O obtained by X-ray Rietveld analysis (XRD) in $La_{1-x}Sr_xMnO_3$ solid solutions. The Mn-O and La-O distances of $LaMnO_3$(x = 0.0) are respectively 1.98 Å and 2.77 Å, which shows good agreement with those derived from ionic radius. The first neighbor Mn-O distance obtained by XAFS continuously decreases from 1.98 Å at x = 0.0 to 1.94 Å at x = 0.4, which is in good accordance with that obtained by XRD. The La(Sr)-O distance obtained by the XRD also decreases from 2.77 Å to 2.74 Å in all the compositional range. However the La-O obtained by the XAFS drastically decreases and becomes 2.67 Å in the compositional range of $0.3 \leq x < 0.4$. This distance is shorter than that obtained by XRD and derived from ionic radius. The Sr-O remained around 2.78 Å in all the compositional range. These facts indicate that the valence state of Mn and the local structure around substituted Sr in La-site was different from those in $LaMnO_3$.

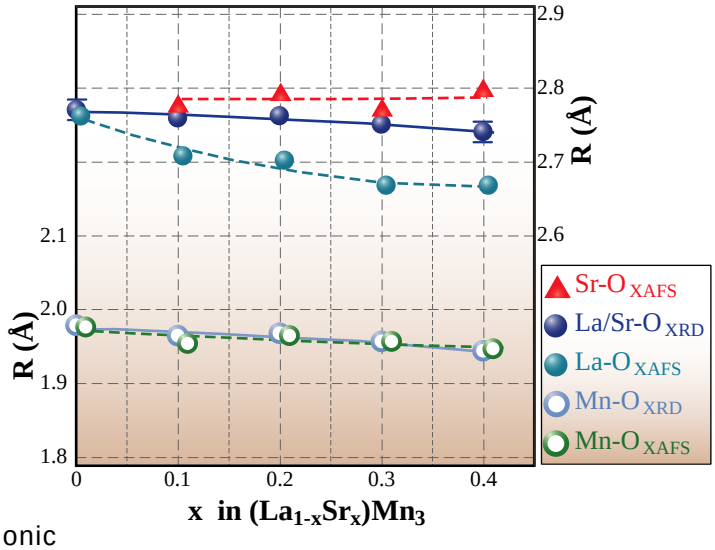

Fig. 6. Compositional dependence of La-O, Sr-O and Mn-O distances in $La_{1-x}Sr_xMnO_3$ solid solutions.

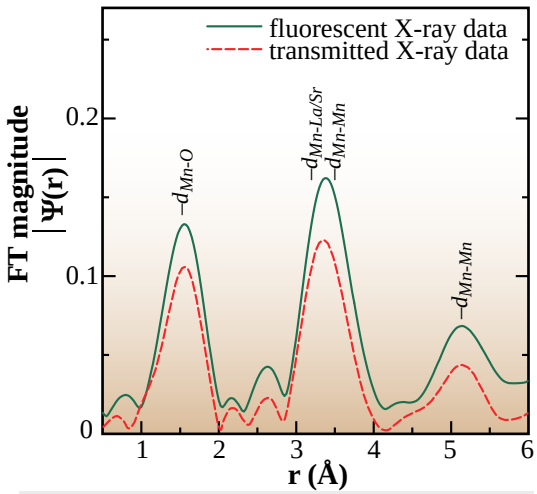

Fig. 5. Fourier transforms of k^3-weighted Mn K-edge XAFS spectra of $La_{0.7}Sr_{0.3}MnO_3$.

Hiroshi Deguchi[a], Akira Mikami[b] and Tohru Yamamoto[c]

(a) Kansai Electric Power Co., INC.
(b) SANYO Electric Co., LTD.
(c) Central Research Institute of Electric Power Industry

E-mail: K422950@kepco.co.jp

References

[1] Y. Hirai, SPring-8 Annual Report 1999 (1999) 100.
[2] Matsushita Technoresearch, INC., Sumitomo Electric Industries, LTD., Toyota Central Research & Develop. Labs., INC., SANYO Electric Co., LTD., Central Research Institute of Electric Power Industry, Kansai Electric Power Co., INC. & Osaka University.
[3] F.W. Lytle *et al.*, Nucl. Instrum. Meth. **226** (1984) 542.